Journal of Applied Polymer Science

Preparation and characterization of polybutylene-succinate/poly(ethylene-glycol)/cellulose nanocrystals ternary composites

Leandro N. Ludueña,[1] Elena Fortunati,[2] Juan I. Morán,[1] Vera A. Alvarez,[1] Viviana P. Cyras,[3] Debora Puglia,[2] Liliana B. Manfredi,[3] Mariano Pracella[4]

[1]Composite Materials Division (CoMP)—National Research Institute of Materials Science and Technology (INTEMA)—National Research Council (CONICET)—National University of Mar del Plata (UNMdP), Solís 7575 (B7608FDQ) Mar del Plata, Argentina
[2]Civil and Environmental Engineering Department—UdR INSTM Strada di Pentima 4 (05100) Terni, University of Perugia, Perugia, Italy
[3]Ecomaterials Division—National Research Institute of Materials Science and Technology (INTEMA)—National Research Council (CONICET)—National University of Mar del Plata (UNMdP), Av. Juan B. Justo 4302, (B7608FDQ), Mar del Plata, Argentina
[4]Institute for Polymers, Composites and Biomaterials (IPCB-CNR)—Department of Civil and Industrial Engineering—University of Pisa, Largo L. Lazzarino 2 (56122), Pisa, Italy
Correspondence to: L. B. Manfredi (E-mail:lbmanfre@fi.mdp.edu.ar)

ABSTRACT: Ternary composites were prepared by twin screw extrusion from polybutylene-succinate (PBS), poly(ethylene-glycol) (PEG), and cellulose nanocrystals (CNC). The aim of the work is to improve the physical–mechanical properties of PBS by the addition of CNC. A PEG/CNC masterbatch was prepared in order to achieve a good dispersion of hydrophilic CNC in the hydrophobic PBS. The influence of the nanoparticle content on the polymer properties was studied. Regarding the thermal properties fractioned crystallization phenomena of PEG was observed during cooling from the melt. No significant nucleating effect of the nanocellulose was observed. The material containing 4 wt % of CNC showed the best mechanical performance among the nanocomposites studied due to the combination of high modulus and elongation at break with a low detrimental in strength compared with the PBS/PEG blend. Moreover, no nanocellulose agglomerations were observed in its FESEM micrograph. © 2015 Wiley Periodicals, Inc. J. Appl. Polym. Sci. **2016**, *133*, 43302.

KEYWORDS: biodegradable; nanoparticles; nanowires and nanocrystals; properties and characterization

Received 13 May 2015; accepted 29 November 2015
DOI: 10.1002/app.43302

INTRODUCTION

The use of conventional plastics has been growing during the last few decades and most of them are non-biodegradable. Consequently, waste matters of plastics contribute to the environmental pollution. This problem has stimulated the interest in developing biodegradable polymers. Nevertheless, the majority of these type of green polymers are not widely used because they are expensive and especially due to its limited properties for specific applications. Among the environmentally friendly biodegradable polymers, polybutylene-succinate is one of the most promising aliphatic polyesters. PBS is becoming increasingly important for new applications in strategic fields such as food packaging and automotive industry. Its potential in the food packaging industry derives from its thermo-mechanical properties that approach it to the hydrocarbon thermoplastic (as polyethylene and polypropylene).[1] Besides, it is a semi-crystalline polymer with good processability and high chemical resistance than other biodegradable plastics.[2,3] PBS is configured as a viable and complementary alternative to other materials derived from renewable sources such as PLA. Compared to this latter, the lower melting point of PBS (110°C) allows a wide range of applications between −20°C and 100°C, while the characteristics of crystallinity and the semi-polar structure give a good rigidity and the possibility to be used in high speed industrial processes. Moreover PBS displays a good permeability, similar to that of PLA.

To improve the mechanical and barrier properties of PBS, were prepared composites with lignocellulosic fibers from coconut, sugar cane, agave, and curauá by means of thermoforming technique. Excellent results were obtained in terms of adhesion at the interface, impact resistance, and elastic modulus, without chemically altering the fibers and thereby developing a material completely "bio."

In the last years, great importance has been given to the development of bionanocomposites containing nanoclay[4] or nanocellulose[5]

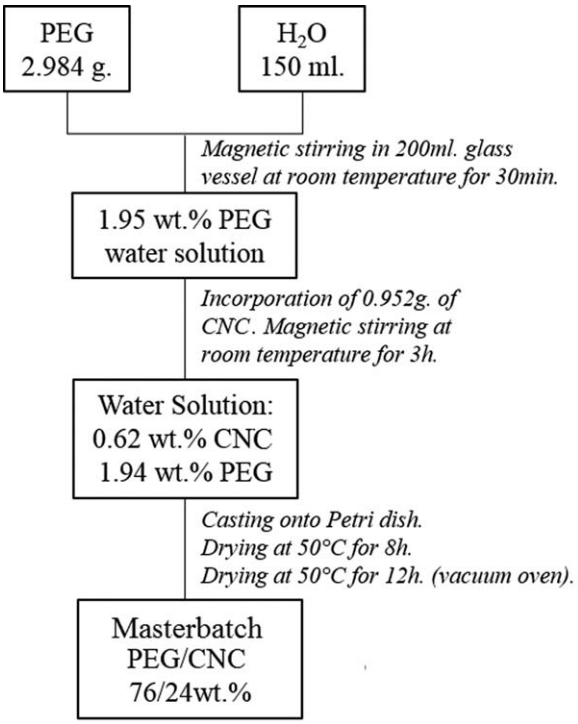

Figure 1. Procedure for the preparation of PEG/CNC masterbatch.

with the aim of improving the mechanical, thermal, and barrier properties of the biopolymers. The idea of using nanocellulose as reinforcement derived from the possibility of taking advantage of the high stiffness and strength of cellulose crystals in composite applications.[6,7] Several approaches for the preparation of highly purified nanocellulose from cellulosic materials have been reported, such as steam explosion treatment, acid or alkaline hydrolysis, enzyme-assisted hydrolysis, as well as a combination of two or several of these methods.[8,9] However, the main problem is the poor dispersion of nanocellulose in the polymeric matrix due to their low compatibility, which may result in lower final properties.[10] Because of this, several strategies were used in order to achieve homogeneous dispersions of nanoparticles in the polymers such as solubilization methods, functionalization, or blending with another polymer.[11]

Bionanocomposites based on biodegradable polyester matrix are recognized of broad scientific and applicative interest in various advanced sectors—as high strength nanopaper, nanocoatings, nanobarriers, cosmetic, and pharmaceutical products, etc.[12,13] Particularly, few examples are reported in the literature in which the nanocellulose was considered as suitable filler for polybutylene–succinate matrix. As an example, Jang[14] studied the effect of microfibrillated cellulose (MFC) content and coupling agent (polymeric methylene diphenyldiisocyanate, pMDI) on the thermal and mechanical properties of MFC-reinforced polybutylene-succinate nanocomposite. Another example was represented by Lin,[15] in which two polysaccharide nanocrystals-rod-like cellulose whisker (CW) and platelet-like starch nanocrystal (SN) were individually incorporated into PBS at loading levels of 2 wt % CW or 5 wt % SN, showing simultaneous enhancement of tensile strength and elongation at break compared to the neat PBS. The good properties of the obtained nanocomposites were attributed to the uniform dispersion of nanofillers and strong interfacial adhesion between filler and matrix. The authors first suspended nanocrystalline cellulose in organic solvents using sonication before blending with the desired polymer, followed by evaporation casting. Moreover another strategy that can be pursued is the blending with another third component. As reported in a previous study on PLA nanocomposites[16] the preparation of nanocomposites of PBS with cellulose nanocrystals is aimed at improving the physical–mechanical performances as well as the biodegradability of PBS, through blending with a compatible polymer (polyethylene glycol, PEG) in order to enhance the dispersion of the nanoparticles within the matrix and the interfacial adhesion, therefore allowing a better control of the morphology and crystallization processes. A water-based PEG/CNC masterbatch was prepared in order to enhance the dispersion of the nanoparticles. The water-assisted technique contributes to a better dispersion of the nanoparticles, without using surface modifiers, and significantly affects the morphology and properties of the resulting nanocomposites.[17] Different percentage of CNC from 2 to 6 wt % were added to the polymeric matrix in order to determine the influence of the nanoparticle content on the properties of PBS and then to choose the material with the best performance.

EXPERIMENTAL

Materials

Polybutylene-succinate (PBS) was purchased, in pellet form, from Showa Denko K.K. under the trade name Bionolle 1001MD. Polyethylene glycol (PEG) (M_n 20,000 g mol^{-1}) was obtained from Aldrich. Microcrystalline cellulose (MCC), supplied by Sigma–Aldrich, was used as start material in cellulose nanocrystal (CNC) synthesis. All the chemical reagents were supplied by Sigma–Aldrich and used as received.

Synthesis of Cellulose Nanocrystals

Commercial microcrystalline cellulose powder (MCC) was hydrolyzed in sulfuric acid hydrolysis (64 wt %) at 45°C for 30 min as previously reported by Fortunati.[18] After removing the acid, dialysis and ultrasonic treatment were performed. The resultant cellulose nanocrystal aqueous suspension was ~0.5 wt % and the yield was nearly 20%. Mixed bed ion exchange resin (Dowex Marathon MR-3 hydrogen and hydroxide form) was added to the cellulose suspension for 24 h and then removed by filtration. This procedure ensured that all ionic materials were removed except the H^+ counter ions associated with the sulfate groups on the CNC surfaces. Finally, the pH of cellulose nanocrystal suspension, before the freeze-drying procedure, was raised to ~9 by using 0.25 wt % NaOH solution, in order to assure the thermal stability of the produced nanocrystals.

Preparation of PEG/CNC Masterbatch

The steps for the preparation of PEG/CNC masterbatch is shown in Figure 1. After casting and drying steps, a fragile PEG/CNC film is obtained. The film was recovered from the Petri dish in order to be melt blended at different proportions with pure PBS. The preparation of the PEG/CNC masterbatch was the critical step for obtaining well dispersed CNCs in the final ternary blends. It is expected to obtain highly dispersed PEG/CNC nanocomposite

Table I. Composition of the PBS/PEG Blend and Nanocomposites

Sample	PBS/PEG/CNC (wt %)
PBS/PEG	80/20/0
CNC2	80/20/2
CNC4	80/20/4
CNC6	80/20/6

masterbatch by solvent (water) casting, which can be subsequently diluted by melt blending with PBS avoiding CNC agglomeration in the process.[19] PEG was selected as a dispersion agent because it is soluble in distilled water and it is miscible with PBS under the melt blending conditions used in this work.[20]

Preparation of PBS/PEG/CNC Nanocomposites

PBS/PEG/CNC nanocomposites were prepared following the proportions showed in Table I. All materials were dried in vacuum oven at 40°C for 48 h before extrusion. The nanocomposites were prepared in a double screw extruder Thermo Scientific Haake Minilab with a capacity of 7 g per extrusion cycle. Extrusion conditions were 155°C, 90 rpm, and 3 min for the barrel temperature, screws rotation speed and residence time, respectively. Residence time was taken after all the materials were inside the extruder. After extrusion, dog bone-shaped samples, in accordance with the ASTM Standard D638-03 Sample Type IV, were prepared by injection molding in a Thermo Scientific Haake Minijet II. Injection conditions were 155°C, 550 bar, 15 s, and 35°C for the furnace-piston temperature, injection pressure, filling time and mold temperature, respectively.

Characterization

Thermal Properties. Thermal degradation measurements were carried out using a TA instruments Auto-MTGA Q500 Hi-Res thermogravimetric analyzer (TGA). Temperature program was run from 25 to 900°C at a 10°C min^{-1} heating rate under nitrogen atmosphere (60 mL min^{-1}). The sample weight in all tests was ~10 mg.

Differential scanning calorimetry experiments were performed on a TA instruments Q2000, at a rate of 10°C min^{-1} under inert nitrogen atmosphere (40 mL min^{-1}). The first heating was performed from −50 to 150°C, the sample was maintained for 10 min at 150°C and then it was cooled to −50°C and the second heating was performed from −50° to 150°C.

The PBS or PEG percentage of crystallinity was calculated according to the eq. (1):

$$X_c(\%) = \frac{\Delta H_m}{w_f \Delta H_m^0} .100 \quad (1)$$

where ΔH_m is the melting enthalpy measured from heating experiments, is the theoretical enthalpy of 100% crystalline polymer (ΔH_m^0 (PBS) = 102J g^{-1} [21]; ΔH_m^0 (PEG) = 208J g^{-1} [21]), w_f is the weight fraction of the polymer in the blend or in the composite.

Fourier Transform Infrared Spectroscopy (FTIR). Spectra were obtained in a Mattson Genesis II, in attenuated total reflection (ATR) mode. A spectral width of 400–4000 cm^{-1}, 16 accumulations, and 2 cm^{-1} resolution was used in the analyses.

X-ray Diffraction Analyses (XRD). XRD analyses were performed with Cu Kα ($\lambda = 1.54$ Å) radiation in a PANalytical X'Pert Pro diffractometer. Every scan was recorded in the range of $2\theta = 2$–60° at a scan speed of 2° min^{-1} with an X-ray tube operated at 40 kV and 40 mA.

Morphology. The morphology of the surface of cryo-fractured samples and the cellulose nanocrystals directly cast onto silicon after hydrolysis were observed by Field Emission Scanning Electron Microscopy (FESEM) Zeiss Supra 25. Prior to the observation, the surfaces were sputter-coated with a gold layer about 100 Å thick to avoid charging under the electron beam.

Mechanical Properties. Tensile tests were performed in a Lloyd Instruments LR30K testing machine. Before tests, all samples were conditioned at 40% relative humidity and 25°C for 48 h. Tests were carried out following the ASTM Standard D638-03. Five injection molded specimens of each formulation were tested for the statistical analysis of the mechanical properties. Crosshead speed was 10 mm min^{-1} (recommended by the ASTM standard). A load cell of 500N was used.

RESULTS AND DISCUSSION

The first derivative of the weight loss curve with respect to temperature (DTG), from TGA tests of the materials are shown in Figure 2. The peak of the first derivative indicates the point of greatest rate of change on the weight loss curve. It can be observed that the maximum thermal degradation rate (T_p) for PBS and PEG takes place at 393 and 410°C, respectively. However, the CNC starts to degrade at lower temperature than the polymers, showing a broad peak in the region between 200 and 500°C. It was previously reported by Fortunati[22] that in the case of cellulose nanocrystals from MCC, after the acid treatment, a substantial change in the degradation profile of raw MCC was

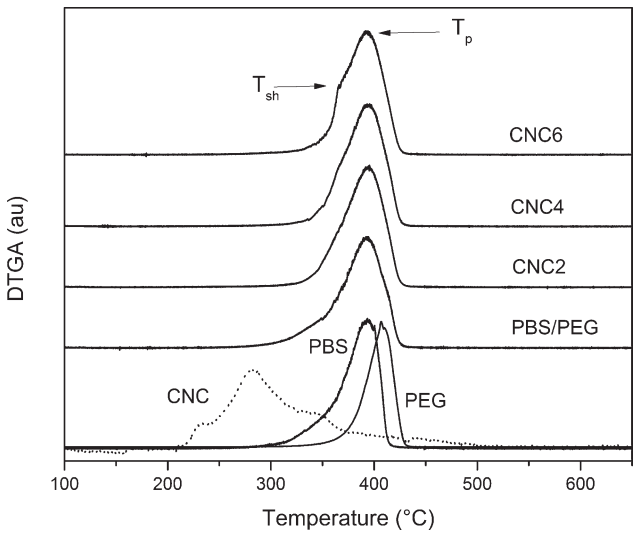

Figure 2. DTG curves of neat PBS, PEG, CNC, PBS/PEG blend, and nanocomposites.

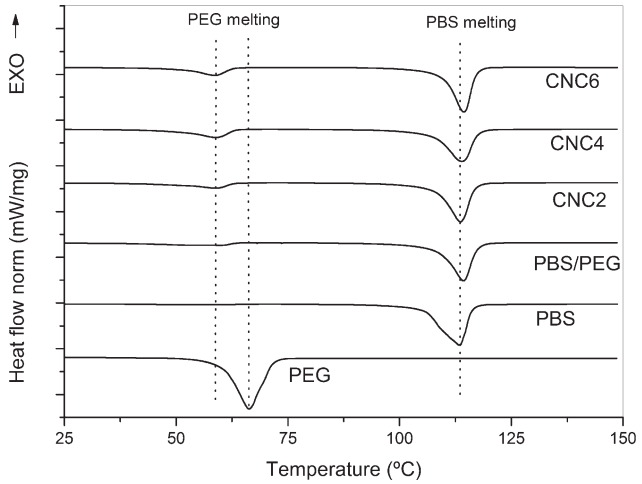

Figure 3. First heating DSC curves of neat PBS, PBS/PEG blend, and nanocomposites.

observed due to the introduction of sulfate groups that diminishes the thermal stability of the cellulose nanocrystals.[23] It has been suggested that the degradation process of highly sulfated samples is best described in terms of two subprocesses: the first subprocess corresponds to the degradation of the more accessible regions, which are highly sulfated, and the second subprocess corresponds to the breakdown of the crystalline fraction which has not been attacked by sulfuric acid. The sample of the PBS/PEG blend showed one broad peak comprising the degradation range of both pure polymers. Moreover, samples containing CNC showed a weak shoulder (T_{sh}) on the left of the main peak that may arise from the thermal degradation of CNC, which is more visible with increasing CNC content. It was observed that although the CNC starts to degrade at 200°C, the nanocomposites are thermally stable up to 300°C. Then, the addition of the masterbach PEG/CNC did not reduce the good thermal stability of the PBS, not affecting their initial and main degradation temperature.

The first heating DSC curves of the pure polymers, blend, and nanocomposites with CNC are shown in Figure 3. The values of melting parameters and crystallinity calculated from the first heating run are reported in Table II for all materials. In the curves of PBS/PEG blend and nanocomposites, two melting peaks were observed at around 113 and 59°C corresponding to the melting of PBS and PEG, respectively. The melting temperature of PBS was neither affected by the addition of PEG in the blend, nor by the CNC content. However, the melting temperature of pure PEG (66°C) was shifted to lower temperatures both in the blend and nanocomposites. Additionally, the PEG crystallization peak was more sharp and narrower in the pure sample. So, it could be assumed that the crystals in the pure PEG are

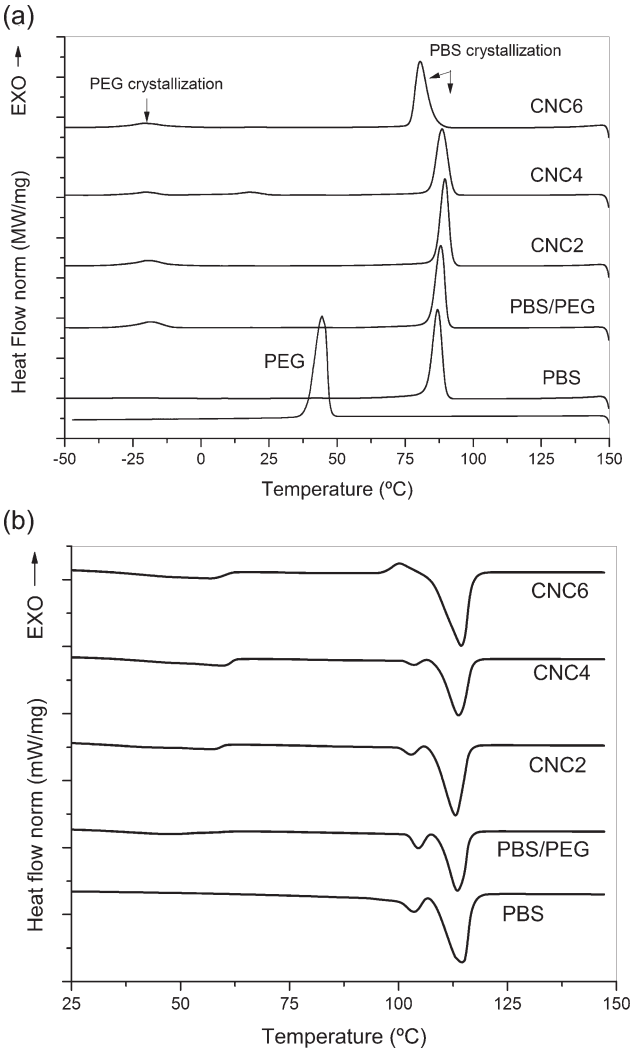

Figure 4. Cooling (a) and second heating (b) DSC curves of neat PBS, PBS/PEG blend, and nanocomposites.

Table II. Thermal Properties of PBS, PEG, their Blend, and Nanocomposites from First DSC Heating Run

	Heating run					
	Melting PEG			Melting PBS		
Sample	T_m (°C)	ΔH (J g^{-1})	%X_c (max 0.2)	T_m (°C)	ΔH (J g^{-1})	%X_c (max 0.8)
PBS	–	–	–	113.4	13.76	13.49
PBS/PEG	60.1	2.78	6.68	114.2	12.29	15.06
CNC2	59.0	3.19	7.82	113.7	11.87	14.84
CNC4	58.8	4.13	10.34	113.9	11.47	14.64
CNC6	58.8	3.44	8.80	114.4	11.55	15.06

Table III. Thermal Properties of PBS, PEG, their Blend, and Nanocomposites from DSC Cooling Run

	Cooling run					
	Crystallization PEG			Crystallization PBS		
Sample	T_c (°C)	ΔH_c (J g^{-1})	%X_c (max 0.2)	T_c (°C)	ΔH_c (J g^{-1})	%X_c (max 0.8)
PBS	–	–	–	86.9	10.53	10.32
PBS/PEG	−18.7	1.68	4.04	88.1	9.51	11.65
CNC2	−19.7	1.87	4.59	89.6	9.62	12.03
CNC4	−20.3	1.59	3.98	88.5	9.02	11.51
CNC6	−20.6	1.58	4.05	80.5	9.40	12.25

more homogeneous than in the blend and in the nanocomposites because the presence of another component during nucleation leads to crystallites varying in sizes and shapes.[24] The percentage of crystallinity of PBS was calculated as a mean value of 13.5%. A slight increment of this value with the addition of PEG can be observed which could be attributed to the plasticizing effect of PEG. On the other hand, a little increment of the crystallinity of PEG was observed when CNC was added to the blend together with a slight diminution in the T_m (Table II), which could be due to a small nucleating effect of CNCs on PEG due to the higher affinity of CNC with PEG than with PBS.[25] This effect was more evident for CNC4, which was observed to be the most homogeneous nanocomposite by FESEM, as explained later.

The DSC cooling curves of the pure components and the composites are summarized in Figure 4 and the relevant thermal parameters (T_c, ΔH_c, and X_c) are listed in Table III. Neat PBS crystallized at higher temperature (86.9°C) than neat PEG (44.4°C). From Figure 4, it is possible to observe that in the PBS/PEG blend, both PBS and PEG components were able to crystallize at a cooling rate of 10°C min^{-1}. There is a little increase of T_c of PBS in the presence of PEG (likely due to the plasticizing effect which enhances the crystal perfection). This is in agreement with the observed parallel increase in crystallinity. The nanocrystals do not influence the nucleation of PBS crystals from the melt, as observed for PLA nanocomposites containing CNC,[16,26] until the incorporation of 6 wt % of CNC, where the T_c was shifted to a lower temperature. This would suggest that a higher amount of CNC is able to restrict the molecular mobility hindering to some extent the crystallization. On the other hand, the crystallization of PEG occurred after complete crystallization of PBS component. The crystallization temperature of PEG showed a similar value in the blend and in the nanocomposites, but it is significantly lower than that of the pure PEG. It's possible that the large decrease of T_c of PEG (together with the decrease of ΔH_c) in the presence of PBS is a consequence of fractionated crystallization phenomena of PEG. The same behavior was observed in PBS/poly (butylene adipate) (PBA) blends[27] where it was stated that the PBS component suppresses the crystallization of PBA due to the physical confinement effect of PBS on the PBA component.

To evaluate the thermal behavior of the materials avoiding the influence of their thermal history a second heating scan was performed after the cooling run. The DSC traces in the second heating run [Figure 4(b)] evidenced the existence of two

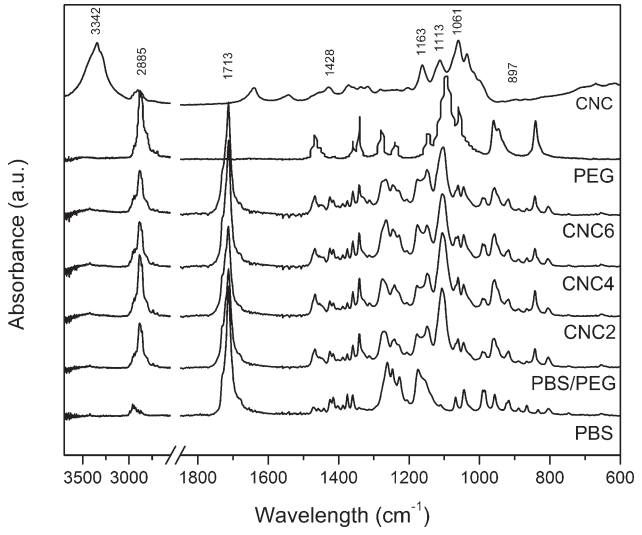

Figure 5. FTIR curves of CNC, PBS, and PBS/PEG blend and nanocomposites.

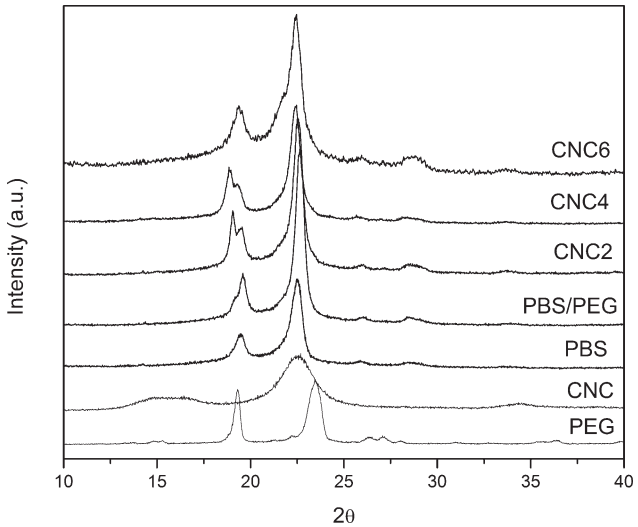

Figure 6. XRD patterns of PBS, PEG, CNC, PBS/PEG blend, and nanocomposites.

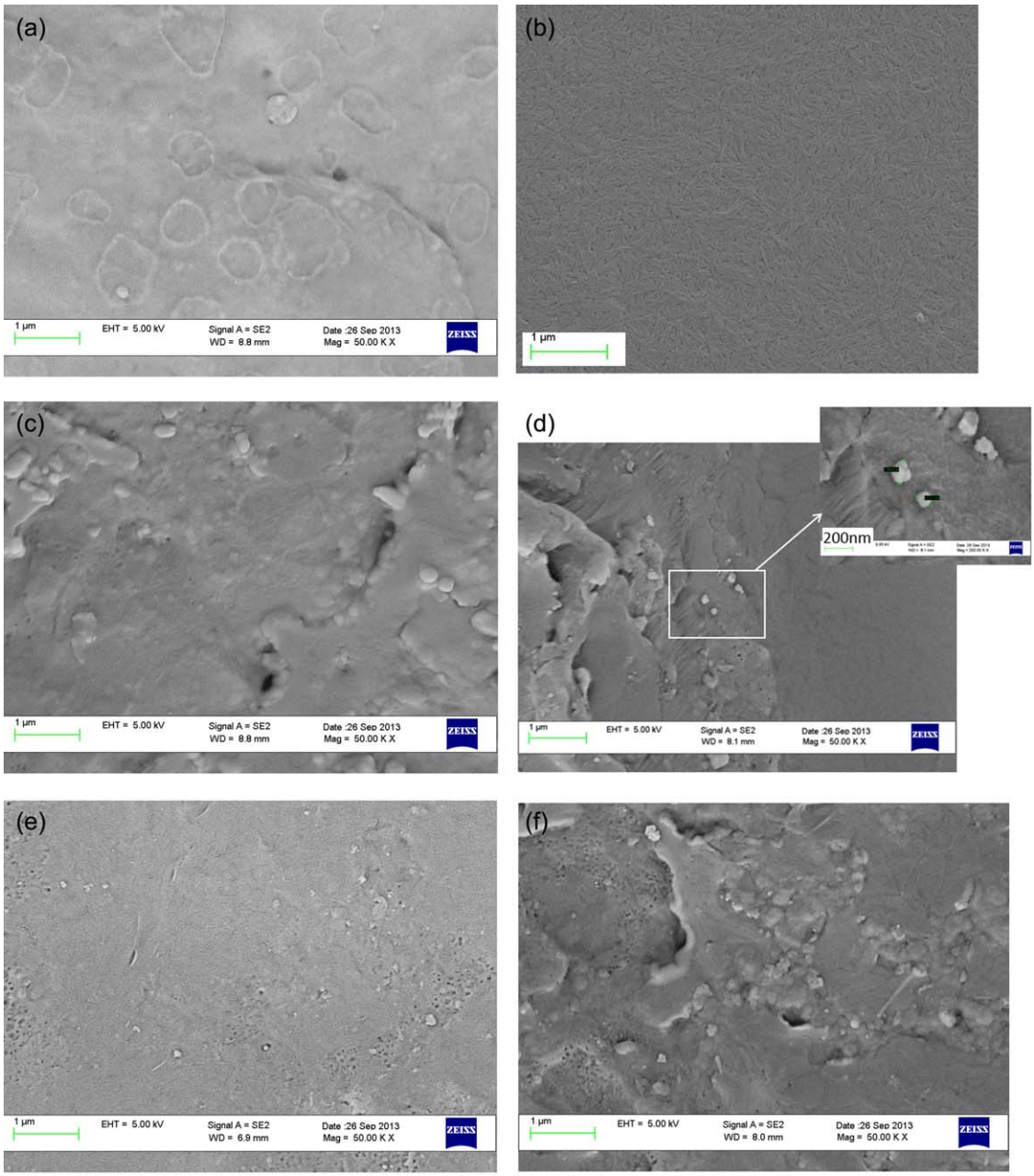

Figure 7. FESEM micrographs of: (a) PBS; (b) CNC; (c) PBS/PEG; (d) CNC2 (with zoom of the agglomerates); (e) CNC4; (f) CNC6. [Color figure can be viewed in the online issue, which is available at wileyonlinelibrary.com.]

melting peaks for the PBS. They are due to the well-known melting-recrystallization-remelting process, also observed in other polyesters such as poly(lactic acid)[28] and poly(hydroxybutyrate).[29] The lower temperature melting peak was attributed to the melting of original crystals, formed before the second DSC scan, and the higher one is associated with the melting of the recrystallized crystals during the heating scan.[30] In the case of the nanocomposite CNC6, the melting peak is preceded by the exotermic peak of crystallization.

The FTIR spectra of the samples are shown in Figure 5. FTIR spectrum of the CNC showed absorption bands that are all typical of cellulosic materials.[31] The spectra analysis confirmed the absence of the 1256 cm^{-1} peak, suggesting the effective removal of hemicelluloses in the hydrolyzed materials.[31] The peak centered at 1428 cm^{-1} is due to the —CH_2— bending. The small, sharp band at 895 cm^{-1} represents glycosidic —C_1—H deformation, with a ring vibration contribution and —OH bending. The peaks at 1061 and 897 cm^{-1} are associated with C—O stretching and C—H rock vibrations of cellulose and the one at 3342cm^{-1} reflects the stretching vibration of O—H.[31] The signal at 871 cm^{-1} can be assigned to the antisymmetric out-of-phase stretching of glucose ring in cellulose, confirming the existence of cellulose nanocrystals (and their monomeric units) after the hydrolysis treatment; moreover, the presence of signals at 1428,

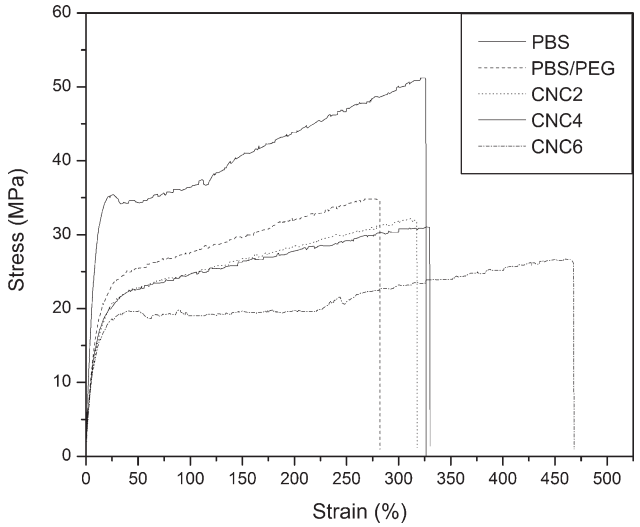

Figure 8. Typical stress–strain curves from tensile tests for neat PBS, PBS/PEG, and its nanocomposites with CNC.

1163, 1113, and 897 cm^{-1} indicated that the CNC are primarily in the form of cellulose I.[32] Native cellulose, called cellulose I, is made of parallel chains that can be organized into two distinct crystalline forms, namely triclinic Iα and monoclinic Iβ, the latter being the more thermodynamically stable.[33]

The spectra of PBS show the characteristic ester absorption peaks at 1713 cm^{-1} for the stretching vibration of the —COO—, and at 1100–1300 cm^{-1} for the stretching vibration of the C—O—C. In the FTIR spectrum of PBS/PEG, the PEG absorption bands at 1100 and 2885 cm^{-1} are characteristic for the stretching of C—O—C and O—CH_2 group, respectively. Additionally, it was observed a slight increase of the nanocomposites peaks in the region 900–1200 and 3300 cm^{-1}, corresponding to the cellulose nanocrystals.

XRD patterns of the materials are shown in Figure 6. The diffraction curves at $2\theta = 19.5$, 21.9, and 22.6° were assigned to (020), (021), and (110) planes of PBS, respectively.[34] On the other hand, two peaks were observed in the pattern of PEG at $2\theta = 19.2$ and 23.5°.[35] Cellulose nanocrystals exhibited four main reflection peaks at $2\theta = 15.0°$, 16.3°, 22.5°, and 34.4°, where the last one less defined can be associated to the cellulose I crystalline structure.[36] The peaks of the PEG and PBS pure components seems to be superimposed in the pattern of the PBS/PEG blend, while a change in the shape and position of the first double peak (at about 19.5°) was observed for the nanocomposites as compared to the blend. Otherwise, the second peak of PBS (at about 22.5°) was not significantly affected. It seems that the addition of CNC did not change the crystalline structure of PBS, but increased the crystallinity of PEG due to the increment observed in the height of the peak at ~19.5°. This result is in accordance to the variation in the percentage of crystallinity measured by DSC (Table II). Additionally, the peaks corresponding to the CNC appeared in the patterns of the nanocomposites and are more clearly seen in the CNC6.

FESEM micrographs of the neat PBS, CNC, PBS/PEG blend, and nanocomposites are shown in Figure 7(a–f). The cellulose micrograph obtained from dried sample [Figure 7(b)] revealed that the nanocrystals are agglomerated into flakes due to strong hydrogen bonds formation. The dimensions of the crystals are in the range from 100 to 200 nm in length and 5–10 nm in width, as reported in a previous work.[22] No evidence of phase separation is observed for PBS/PEG blend in Figure 7(c). Small aggregates with spherical shape and size around 150 nm were observed in the micrographs of the nanocomposites with 2 and 6 wt % of CNC [Figure 7(d,f)], but a quite homogeneous CNC dispersion were found in the nanocomposites with 4 wt % of CNC [Figure 7(e)]. So, the nanoparticles were almost homogeneously dispersed inside the polymeric matrix because FESEM analysis did not reveal the presence of nanocellulose micro agglomerates.

Typical stress–strain curves obtained in tensile tests for neat PBS, PBS/PEG, and its nanocomposites with CNC are shown in Figure 8. It is possible to observe that all the materials exhibited an initial linear behavior followed by a nonlinear part, indicative of the plastic deformation. The results of mechanical tests (Young's modulus, maximum tensile strength, and elongation at break) of all tested samples are reported in Table IV. As it was expected, blending PBS with a polymer such as PEG, showing low stiffness, strength, and ductility, worsen the mechanical behavior of the neat PBS reducing their modulus and tensile strength. Regarding the nanocomposites the sample containing 4 wt % of CNC displayed a modulus ~16% higher than that of PBS/PEG blend. Nevertheless, the composites CNC2 and CNC6 did not show such improvement probable due to the poorer dispersion of the CNC in the polymer blend, as was observed by FESEM. Another factor affecting the modulus value of CNC4 could be the crystallinity of the PEG that was observed to increase somewhat in that sample by DSC. On the other hand, no enhancement in the tensile strength with increasing filler loading was found. Fu[37] reported that composite strength and toughness are significantly affected by the particle/matrix adhesion quality. The adhesion strength at the interface determines the load transfer between the components, so a strong interfacial bonding between particles and polymer matrix is critical for effective stress transfer leading to high composite strength. So, it seems that it was not reached as high as expected adhesion between the particles and the matrix, especially at higher loadings (CNC6) which displayed the greatest diminution in strength. Moreover, an increase in the elongation and a diminution in strength with the CNC content was

Table IV. Mechanical Properties of the Neat PBS, PBS/PEG Blend, and Nanocomposites

Sample	Young's modulus (MPa)	Maximum tensile stress (MPa)	Elongation at break (%)
PBS	536 ± 30	50.6 ± 1.3	326 ± 23
PBS/PEG	336 ± 27	36.0 ± 1.7	283 ± 28
CNC2	339 ± 22	32.3 ± 0.2	320 ± 18
CNC4	391 ± 13	31.6 ± 0.4	329 ± 33
CNC6	325 ± 16	26.8 ± 0.4	482 ± 62

observed. Similar behavior was reported by Mandal[24] who studied nanocomposites of PVA/nanocellulose. They explain this behavior considering that CNC could hinder to some extent the formation of hydrogen bonds amongst PVA chains thus loosing tensile strength but gaining ductility with the CNC content. They also consider that the nanocellulose, a good carrier of water, plasticizes the polymer matrix thus increasing the elongation at break. In a similar trend it could be possible to explain the effect of CNC on PEG. Additionally, the ultimate strength of a composite depends on the weakest fracture path throughout the material. So, it is difficult to predict the strength of composites because the particles affect the strength weakening due to the stress concentration they cause, but also reinforcing because they may serve as barriers to crack growth. To summarize, it seems that the sample CNC4 showed the best performance among the nanocomposites studied due to its high modulus with a low detrimental in maximum strength compared to the PBS/PEG blend. Additionally, it was improved the elongation at break of the blend.

CONCLUSIONS

Homogeneous nanocomposite films from PBS/PEG and cellulose nanocrystals were successfully obtained by twin screw extrusion. The use of a PEG/CNC masterbatch was the strategy proposed for allowing a good dispersion of hydrophilic CNC in the hydrophobic PBS polymeric matrix.

It was found that the addition of CNC did not diminish the thermal resistance of the PBS/PEG blend and did not modify the crystalline structure of PBS.

A slight plasticizing effect of PEG due to the small increment in the crystallization temperature (T_c) and crystallinity of PBS during the DSC cooling test from the melt was observed. Additionally, a fractioned crystallization phenomenon of PEG was observed due to the notable diminution of its T_c. No significant nucleating effect of the nanocellulose was observed.

The effect of the CNC amount on the mechanical properties of the PBS/PEG blend was also analyzed. It was observed that the sample CNC4 showed the best mechanical performance among the nanocomposites studied due to the combination of high modulus and higher elongation at break than the PBS/PEG blend. Besides, a more homogeneous dispersion of the CNC was observed by FESEM analysis of the nanocomposites.

ACKNOWLEDGMENTS

The authors are grateful to the National Research Council of Argentina (CONICET), International Cooperation Project CNR-CONICET No. 1010, PIP 0014 and 0527, the National Agency of Scientific and Technological Promotion of Argentina (PICT'12 1983), and the National University of Mar del Plata for the financial funding of this research.

REFERENCES

1. Uesaka, T.; Nakane, K.; Maeda, S.; Ogihara, T.; Ogata, N. *Polymer* **2000**, *41*, 8449.
2. Okamoto, K.; Ray, S. S.; Okamoto, M. *J. Polym. Sci. B: Polym. Phys.* **2003**, *41*, 3160.
3. Chen, G. X.; Kim, E. S.; Yoon, J. S. *J. Appl. Polym. Sci.* **2005**, *98*, 1727.
4. Bordes, P.; Pollet, E.; Avérous, L. *Progr. Polym. Sci.* **2009**, *34*, 125.
5. Lee, K.-Y.; Aitomäki, Y.; Berglund, L. A.; Oksman, K.; Bismarck, A. *Compos. Sci. Technol.* **2014**, *105*, 15.
6. Khan, A.; Khan, R. A.; Salmieri, S.; Le Tien, C.; Riedl, B.; Bouchard, J.; Chauve, G.; Tan, V.; Kamal, M. R.; Lacroix, M. *Carbohydr. Polym.* **2012**, *90*, 1601.
7. Dadashi, S.; Mousavi, S.; Emam-Djomeh, Z.; Oromiehie, A. *Iran. J. Polym. Sci. Technol.* **2012**, *25*, 127.
8. Morán, J. I.; Alvarez, V. A.; Cyras, V. P.; Vazquez, A. *Cellulose* **2008**, *15*, 149.
9. Chen, W. S.; Yu, H. P.; Liu, Y. X.; Chen, P.; Zhang, M. X.; Hai, Y. F. *Carbohydr. Polym.* **2011**, *83*, 1804.
10. Petersson, L.; Oksman, K. *Compos. Sci. Technol.* **2006**, *66*, 2187.
11. Peponi, L.; Puglia, D.; Torre, L.; Valentini, L.; Kenny, J. M. *Mater. Sci. Eng. R* **2014**, *85*, 1.
12. Moon, R. J.; Martini, A.; Nairn, J.; Simonsen, J.; Youngblood, J. *Chem. Soc. Rev.* **2011**, *40*, 3941.
13. Luong, N. D.; Pahimanolis, N.; Hippi, U.; Korhonen, J. T.; Ruokolainen, J.; Johansson, L. S.; Nam, J. D.; Seppälä, J. *J. Mater. Chem.* **2011**, *21*, 13991.
14. Jang, J. H.; Lee, S. H.; Kim, N. H. *J. Korean Wood Sci. Technol.* **2014**, *42*, 483.
15. Lin, N.; Yu, J.; Chang, P. R.; Li, J.; Huang, J. *Polym. Compos.* **2011**, *32*, 472.
16. Pracella, M.; Haque, M. M.; Ul., Puglia, D. *Polymer* **2014**, *55*, 3720.
17. Karger-Kocsis, J.; Kmetty, Á.; Lendvai, L.; Drakopoulos, S.; Bárány, T. *Materials* **2015**, *8*, 72.
18. Fortunati, E.; Armentano, I.; Zhou, Q.; Iannoni, A.; Saino, E.; Visai, L.; Berglund, L. A.; Kenny, J. M. *Carbohydr. Polym.* **2012**, *87*, 1596.
19. Haque, M. M.-U. PhD thesis, University of Pisa: Italy, **2012**.
20. He, Z.; Liang, Y.; Wang, P.; Han, C. C. *Polymer* **2013**, *54*, 2355.
21. He, Y.; Zhu, B.; Kai, W.; Inoue, Y. *Macromolecules* **2004**, *37*, 3337.
22. Fortunati, E.; Puglia, D.; Luzi, F.; Santulli, C.; Kenny, J. M.; Torre, L. *Carbohydr. Polym.* **2013**, *97*, 825.
23. Roman, M.; Winter, W. T. *Biomacromolecules* **2004**, *5*, 1671.
24. Mandal, A.; Chakrabarty, D. *J. Ind. Eng. Chem.* **2014**, *20*, 462.
25. Fortunati, E.; Luzi, F.; Puglia, D.; Dominici, F.; Santulli, C.; Kenny, J. M.; Torre, L. *Eur. Polym. J.* **2014**, *56*, 77.
26. Kowalczyk, M.; Piorkowska, E.; Kulpinski, P.; Pracella, M. *Compos. A* **2011**, *42*, 1509.
27. Yang, J.; Pan, P.; Hua, L.; Xie, Y.; Dong, T.; Zhu, B.; Inoue, Y.; Feng, X. *Polymer* **2011**, *52*, 3460.
28. Masirek, R.; Kulinski, Z.; Chionna, D.; Piorkowska, E.; Pracella, M. *J. Appl. Polym. Sci.* **2007**, *105*, 255.

29. D'Amico, D. A.; Manfredi, L. B.; Cyras, V. P. *J. Appl. Polym. Sci.* **2012**, *123*, 200.
30. Gunaratne, L. M. W. K.; Shanks, R. A. *Eur. Polym. J.* **2005**, *41*, 2980.
31. Alemdar, A.; Sain, M. *Bioresour. Technol.* **2008**, *99*, 1664.
32. Leung, A. C. W.; Hrapovic, S.; Lam, E.; Liu, Y.; Male, K. B.; Mahmoud, K. A.; Luong, J. H. T. *Small* **2011**, *7*, 302.
33. Atalla, R. H.; VanderHart, D. L. *Science* **1984**, *223*, 283.
34. Leroux, F.; Dalod, A.; Hennous, M.; Sisti, L.; Totaro, G.; Celli, A.; Coehlo, C.; Verney, V. *Appl. Clay Sci.* **2014**, *100*, 102.
35. Khanna, L.; Verma, N. K. *Phys. B* **2013**, *427*, 68.
36. Fortunati, E.; Peltzer, M.; Armentano, I.; Torre, L.; Jiménez, A.; Kenny, J. M. *Carbohydr. Polym.* **2012**, *90*, 948.
37. Fu, S.-Y.; Feng, X.-Q.; Lauke, B.; Mai, Y.-W. *Compos. B Eng.* **2008**, *39*, 933.